Since January 2020 Elsevier has created a COVID-19 resource centre with free information in English and Mandarin on the novel coronavirus COVID-19. The COVID-19 resource centre is hosted on Elsevier Connect, the company's public news and information website.

Elsevier hereby grants permission to make all its COVID-19-related research that is available on the COVID-19 resource centre - including this research content - immediately available in PubMed Central and other publicly funded repositories, such as the WHO COVID database with rights for unrestricted research re-use and analyses in any form or by any means with acknowledgement of the original source. These permissions are granted for free by Elsevier for as long as the COVID-19 resource centre remains active.

Science of the Total Environment 825 (2022) 153906

Contents lists available at ScienceDirect

Science of the Total Environment

journal homepage: www.elsevier.com/locate/scitotenv

Detection of SARS-CoV-2 RNA throughout wastewater treatment plants and a modeling approach to understand COVID-19 infection dynamics in Winnipeg, Canada

Kadir Yanaç [a], Adeola Adegoke [b], Liqun Wang [b], Miguel Uyaguari [c], Qiuyan Yuan [a,*]

[a] Department of Civil Engineering, University of Manitoba, Winnipeg, Canada
[b] Department of Statistics, University of Manitoba, Winnipeg, Canada
[c] Department of Microbiology, University of Manitoba, Winnipeg, Canada

HIGHLIGHTS

- SARS-CoV-2 RNA is first detected in wastewater on September 30th, 2020, in Winnipeg.
- SARS-CoV-2 RNA may predominate in wastewater solids.
- SARS-CoV-2 RNA is not detected in secondary- and tertiary-treated wastewater.
- SARS-CoV-2 RNA levels in wastewater are sensitive to the fluctuations in infection dynamics.
- Wastewater surveillance can reveal the true scale of a COVID-19 outbreak.

GRAPHICAL ABSTRACT

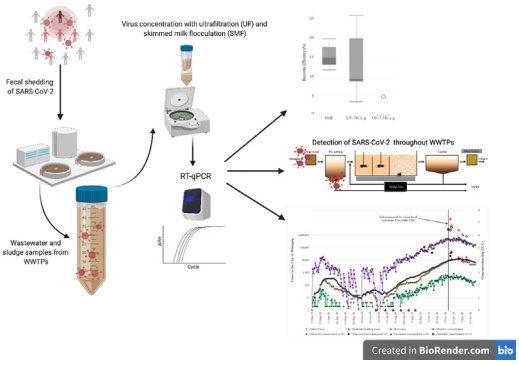

ARTICLE INFO

Article history:
Received 10 October 2021
Received in revised form 4 February 2022
Accepted 11 February 2022
Available online 23 February 2022

Editor: Thomas Kevin V

Keywords:
SARS-CoV-2
Virus concentration
Wastewater solids
Wastewater surveillance
Back-trajectory modeling

ABSTRACT

Although numerous studies have detected SARS-CoV-2 RNA in wastewater and attempted to find correlations between the concentration of SARS-CoV-2 RNA and the number of cases, no consensus has been reached on sample collection and processing, and data analysis. Moreover, the fate of SARS-CoV-2 in wastewater treatment plants is another issue, specifically regarding the discharge of the virus into environmental settings and the water cycle. The current study monitored SARS-CoV-2 RNA in influent and effluent wastewater samples with three different concentration methods and sludge samples over six months (July to December 2020) to compare different virus concentration methods, assess the fate of SARS-CoV-2 RNA in wastewater treatment plants, and describe the potential relationship between SARS-CoV-2 RNA concentrations in influent and infection dynamics. Skimmed milk flocculation (SMF) resulted in 15.27 ± 3.32% recovery of an internal positive control, Armored RNA, and a high positivity rate of SARS-CoV-2 RNA in stored wastewater samples compared to ultrafiltration methods employing a prefiltration step to eliminate solids in fresh wastewater samples. Our results suggested that SARS-CoV-2 RNA may predominate in solids, and therefore, concentration methods focusing on both supernatant and solid fractions may result in better recovery. SARS-CoV-2 RNA was detected in influent and primary sludge samples but not in secondary and final effluent samples, indicating a significant reduction during primary and secondary treatments. SARS-CoV-2 RNA was first detected in influent on September 30th, 2020. A decay-rate formula was applied to estimate initial concentrations of late-processed samples with SMF. A model based on shedding rate and new cases was applied to estimate SARS-CoV-2 RNA concentrations

* Corresponding author.
E-mail address: qiuyan.yuan@umanitoba.ca (Q. Yuan).

http://dx.doi.org/10.1016/j.scitotenv.2022.153906
0048-9697/© 2022 Elsevier B.V. All rights reserved.

and the number of active shedders. Inferred sensitivity of observed and modeled concentrations to the fluctuations in new cases and test-positivity rates indicated a potential contribution of newly infected individuals to SARS-CoV-2 RNA loads in wastewater.

1. Introduction

After the initial detection of COVID-19 in December 2019 in Wuhan, China, the disease has rapidly spread and caused significant health, economic and social burden worldwide. Considering the rapid transmission and spread of COVID-19 and the subsequent emergence of new waves and variants, surveillance of the disease is vital to early predict and control outbreaks in communities. Standard diagnostic testing among populations is challenging due to the time and cost of testing massive numbers of individuals. Moreover, undiagnosed and unreported asymptomatic and mildly symptomatic cases of COVID-19 constitute a significant proportion of infections (Bi et al., 2021; Day, 2020; Ing et al., 2020), which increases the complexity of assessing the true scale of a community outbreak. With the first detection of SARS-CoV-2 RNA in urban wastewater reported in the Netherlands in March 2020 (Medema et al., 2020a), wastewater-based epidemiology (WBE) has emerged as an additional surveillance tool to mitigate these challenges and provide rapid information to government agencies, civil society organizations, and private or public utilities. WBE can be used to determine the effectiveness of public health control measures and the required level of societal restrictions (Bivins et al., 2020b; Hill et al., 2021; Thompson et al., 2020). Moreover, SARS-CoV-2 can remain viable in wastewater for up to 4–5 days (Bivins et al., 2020a; Nghiem et al., 2020), and therefore it may pose health risks to the workers in WWTPs for aggressive and extreme scenarios (Dada and Gyawali, 2021; Zaneti et al., 2021).

WBE has been used as a surveillance and predictive tool to provide near-real-time information on the usage of illegal drugs (Bishop et al., 2020; Sulej-Suchomska et al., 2020) and the prevalence of viral (Bisseux et al., 2018; Ivanova et al., 2019; McCall et al., 2020; Nakamura et al., 2015) and bacterial diseases (Diemert and Yan, 2020; Yan et al., 2018). The presence of SARS-CoV-2 gene fragments in the feces of both symptomatic and asymptomatic infected individuals (Gupta et al., 2020; Jones et al., 2020; Pan et al., 2020) makes wastewater surveillance of COVID-19 a unique epidemiological tool to monitor infection trends in communities and support public health interventions. Indeed, since the onset of COVID-19, many researchers have reported the detection and quantitation of SARS-CoV-2 RNA in wastewater (Ahmed et al., 2020a; D'Aoust et al., 2021; Graham et al., 2021; Medema et al., 2020a; Westhaus et al., 2021). Several potential uses of the generated data include tracking trends temporally to project future infection trajectories (Medema et al., 2020b) and estimating COVID-19 prevalence in a community based on SARS-CoV-2 RNA concentration in wastewater (Ahmed et al., 2020a; Gerrity et al., 2021; Wu et al., 2022). Moreover, considering the partitioning of enveloped viruses to the wastewater solids (Ye et al., 2016), primary sludge and solid phase of wastewater have also been investigated for the wastewater surveillance of COVID-19 (Graham et al., 2021; Peccia et al., 2020). However, operational parameters of primary sedimentation, such as hydraulic retention time, the concentration of total solids, and recirculation of returned/waste activated sludge, may affect the reliability of the measured SARS-CoV-2 RNA concentrations daily. Therefore, the focus should be on both solid and aqueous phases of wastewater rather than primary sludge. In fact, processing sludge and solids samples using reverse-transcriptase quantitative polymerase chain reaction (RT-qPCR) (Peccia et al., 2020) is not as labor-intensive as processing wastewater influent samples, in which viral particles are concentrated either using filtration methods or organic flocculation methods (Ahmed et al., 2020c; Barril et al., 2021). However, regardless of the surveillance type, there are still some methodological questions on the cumulative interpretation of data generated from wastewater analysis and epidemiological data together.

The fate of coronaviruses in environmental compartments can become more of an issue (Carducci et al., 2020) since SARS-CoV-2 in wastewater and aquatic environment can be viable for up to 4 days at room temperatures (Bivins et al., 2020a; Sala-Comorera et al., 2021). Most studies have focused on SARS-CoV-2 RNA concentrations in WWTPs rather than viable SARS-CoV2. Westhaus et al. (2021) detected SARS-CoV-2 RNA in treated wastewater, indicating its potential distribution into aquatic ecosystems, while Hasan et al. (2021) could not detect SARS-CoV-2 RNA in treated wastewater. Detection of SARS-CoV-2 RNA in wastewater solids and sludge (Balboa et al., 2021; D'Aoust et al., 2021; Graham et al., 2021; Peccia et al., 2020) might indicate the predominance of SARS-CoV-2 in solids and sludge line as the primary removal mechanism in WWTPs. The predominance of SARS-CoV-2 in solids can be associated with high loads of SARS-CoV-2 in stool samples/fecal matter (Benefield et al., 2020; Chen et al., 2020; Wölfel et al., 2020). Thus, concentration methods focusing on the recovery from both solids and supernatant may better approach the true concentrations of SARS-CoV-2 RNA in wastewater (Chik et al., 2021). Different wastewater treatment processes, sewage characteristics, and climate conditions may affect the fate of SARS-CoV-2 RNA and viable SARS-CoV-2 in WWTPs. More in-depth investigations will provide better insights into the fate of SARS-CoV-2 throughout WWTPs and its circulation in the water cycle.

There are numerous studies investigating virus concentration methods and wastewater surveillance of SARS-CoV-2 RNA. However, further elucidation of virus concentration methods and detection and quantification of SARS-CoV-2 RNA in relation to COVID-19 infection dynamics will significantly contribute to the current body of knowledge considering the focus of this study on wastewater solids. In this context, different concentration methods were evaluated to investigate the effects of the inclusion of wastewater solids in virus concentration methods on recovery efficiency. Moreover, the relationships between SARS-CoV-2 RNA detection and concentration and COVID-19 infection dynamics using a back-trajectory modeling approach were examined.

2. Materials and methods

2.1. Sample collection

One-liter of 24-h flow-proportional composite raw wastewater samples were collected from three major WWTPs in Winnipeg, Canada, between July 8 and December 15, 2020. These WWTPs are the North End Sewage Treatment Plant (NESTP), South End Sewage Treatment Plant (SESTP), and West End Sewage Treatment Plant (WESTP). Primary sludge (50 mL), secondary effluent (1 L), and final effluent (1 L) grab samples were also collected during this period. Detailed information on sampling dates, sample types, and treatment processes of WWTPs and their design capacities is provided in Table S1 and Table S2, respectively. NESTP and SESTP employ high-purity oxygen (HPO) wastewater treatment systems followed by UV disinfection, while WESTP employs anaerobic/anoxic/oxic (A2O) wastewater treatment system followed by natural light disinfection in the summer and cooling in the winter. Some of the waste activated sludge is recirculated to the primary clarifiers at the NESTP and SESTP, while activated sludge is not recirculated to the primary clarifier at the WESTP. The operators provided daily flowrate (Fig. S1) and wastewater characteristics data. After sampling, wastewater and sludge samples were transported to the laboratory in amber HDPE bottles in an icebox and processed within 24 h.

2.2. Virus concentration assays

Three different virus concentration methods were applied: ultrafiltration at two different centrifugation speeds and skimmed milk flocculation (SMF).

2.3. Ultrafiltration

Samples were processed within 24 h of collection. Raw wastewater, and secondary and final effluent samples (120 mL each) were filtered through cheesecloth and low-protein binding 0.45 and 0.2 μm 47-mm Supor-200 membrane disc filters (Pall Corporation, Ann Harbor, MI), respectively, to remove large particles, sediments, eukaryotes, and bacteria (Uyaguari-Diaz et al., 2016). Solids retained on the filters were stored at −20 °C.

2.3.1. Sequential ultrafiltration at 3000g (UF-3k ×g)

A total of 120 mL of the sample was first concentrated, at 3000*g* for 30 min by loading 60 mL of the sample twice, to approximately 5 mL using Jumbosep Centrifugal Device, 30-kDa (Pall Corporation, Ann Harbor, MI, USA). Then, the 5 mL concentrate was further concentrated down at 3000*g* for 30 min using Microsep Advance Centrifugal Device, 30-kDa, (Pall Corporation, Ann Harbor, MI, USA). The final volume of the concentrate varied between 500 and 1200 μL.

2.3.2. Sequential ultrafiltration at 7500g (UF-7.5k ×g)

To get smaller final volumes and as per the manufacturer's recommendation, centrifugation speed for Microsep was changed from 3000*g* to 7500*g* from October 28th, 2020.

Samples collected between October 28th and December 15th were processed with both UF-3k ×*g* and UF-7.5k ×*g* methods.

2.4. Skimmed milk flocculation

The samples collected between November 16th and December 15th were additionally concentrated by applying SMF protocol (Calgua et al., 2008) even though a long time (Table 1) had passed since the sample collection. The information regarding solids concentrations of the samples is given in Table S4. The influent samples used for SMF recovery efficiency tests were the previously collected and stored samples (storage time > 40 days). Briefly, 0.5 g of skim milk powder (Difco Laboratories, Sparks, MD, USA) was dissolved in 50 mL synthetic seawater (Sigma-Aldrich, St. Louis, MO, USA) to obtain 1% (w/v) skimmed milk solution and pH of the solution was carefully adjusted with 1 M HCl to 3.5. Five mL of skimmed milk solution was added to 500 mL raw wastewater samples. pH of samples was also previously adjusted to 3.5 with 1 M HCl to obtain a final concentration of skimmed milk at 0.01% (w/v). Samples were stirred for 8 h, and flocs were allowed to settle for another 8 h at room temperature. Supernatants were carefully removed using serological pipets without disturbing the settled flocs. A final volume of 50 mL containing the flocs was transferred to centrifuge tubes and centrifuged at 8000 ×*g* for 30 min. Pellets were carefully scraped using a sterilized spatula, and the remaining pellets in the tubes were resuspended in 250 μL of 0.2 M sodium phosphate buffer with a pH 7.5 (Alfa Aesar, Ottawa, ON, Canada) and transferred to 1.5 mL Eppendorf tubes.

2.4.1. Recovery efficiency

Total recovery for ultrafiltration and SMF method workflows were determined by spiking 5×10^4 copies of Armored RNA Quant IPC-1 Processing Control (Asuragen, Austin, TX, USA) (Alygizakis et al., 2021; Eveleigh et al., 2019; Hietala and Crossley, 2006) into six fresh wastewater samples for ultrafiltration method and six stored wastewater samples (storage time > 40 days) SMF method and then stirring and inoculating the samples at 4 °C for 30 min. The samples were collected from North End Sewage Treatment Plant (NESTP), South End Sewage Treatment Plant (SESTP) and West End Sewage Treatment Plant (WESTP) in Winnipeg. The volumes of wastewater samples spiked were 140 and 500 mL for ultrafiltration and SMF methods, respectively. Recovery efficiency percentage was calculated by dividing the recovered concentration by the spiked concentration.

Table 1
Delay in sample processing collected from NESTP, SESTP, and WESTP.

Sampling date	Delay in sample processing (days)
November 16, 2020	75
November 18, 2020	73
December 1, 2020	60
December 8, 2020	53
December 15, 2020	46

2.5. Viral RNA extraction

Viral concentrates from wastewater samples and recovery efficiency assays were processed using the RNeasy PowerMicrobiome Kit (Qiagen Sciences, Inc., Germantown, MD, USA). Phenol:chloroform:isoamyl alcohol 25:24:1 (Invitrogen, Carlsbad, CA, USA) and β-mercaptoethanol (Fisher Scientific, Fair Lawn, NJ, USA) were also added during extraction according to the manufacturer's instructions to improve extraction efficiency. 300 μL of sludge samples were added directly to the beading tubes to extract viral RNA from sludge using the same extraction kit and following the same instructions. Finally, RNA was eluted in 50 μL of elution buffer. Information regarding the solid content of the samples is given in Table S5.

On the other hand, viral RNA was extracted from wastewater solids using MagMAX Microbiome kit (Thermo Fisher, Waltham, MA, USA) following the manufacturer's instructions that included the addition of Proteinase K. The wastewater solids are the solids retained on the filters during prefiltration of influent samples for the ultrafiltration. These filters were stored at −20 °C until extraction. The solids were extracted from the filters by adding 15 mL PBS-0.05% tween-20 solution and vortexing for 10 min. The extracted solids were centrifuged at 3300 ×*g* for 15 min, and pellets were used for RNA extraction. The information regarding total solids and total suspended solids of the wastewater samples is given in Table S4. The RT-qPCR analysis was conducted following the extraction, and extracts were stored at −80 °C.

2.6. RT-qPCR analysis

In this study, N1 and N2 primers/probe sets (Integrated DNA Technologies, Inc., Coralville, IA, USA), each targeting a different region of the Nucleocapsid (N) gene of SARS-CoV-2 (CDC, 2020), were used. Each 10-μL RT-qPCR mixture consisted of 10 μL of 2.5 μL of 4× TaqMan Fast Virus 1-Step Master Mix (Life Technologies, Carlsbad, CA, USA), 400 nM each primer, 250 nM probe, 2.5 μL of the template and ultrapure DNAse/RNAse free distilled water (Promega Corporation, Fitchburg, WI, USA). Calibration curves for quantifying N1 and N2 specific assays were obtained using six 10-fold dilutions (ranging from 2.0 to 2.0×10^5 copies) of the 2019-nCoV_N_Positive Control plasmid DNA (Integrated DNA Technologies, Inc., Coralville, IA, USA). Armored RNA was quantified using 10-fold dilutions of synthetic single-stranded DNA (Integrated DNA Technologies, Inc., Coralville, IA, USA). Primers and probe sets (Integrated DNA Technologies, Inc., Coralville, IA, USA) used to detect and quantify the Armored RNA are given in Table S3. Calibration curves were obtained for each RT-qPCR run. Negative controls were also included in each qPCR run. Standards, samples, and non-template controls were run in triplicate. Thermal cycling reactions were performed at 50 °C for 5 min, followed by 45 cycles of 95 °C for 10 s and 60 °C for 30 s on a QuantStudio 5 Real-Time PCR System (Life Technologies, Carlsbad, CA, USA). Following recommendations by the CDC's (2020) protocol for detection of SARS-CoV-2 RNA if the C_T was <40, samples were considered SARS-CoV-2 RNA positive.

The concentration of SARS-CoV-2 RNA in wastewater in Winnipeg was normalized by dividing daily total SARS-CoV-2 RNA load in wastewater by the total daily wastewater flow rate (Eq. 1). The normalization was implemented for the three WWTPs using Eq. 1, where NC is normalized concentration on a daily basis, C represents the SARS-CoV-2 concentration, and WF indicates the daily wastewater flow.

$$NC = \frac{(C \text{ at NESTP} * WF \text{ to NESTP}) + (C \text{ at SESTP} * WF \text{ to SESTP}) + (C \text{ at WESTP} * WF \text{ to WESTP})}{\text{Sum of WF to NESTP, SESTP, WESTP}} \quad (1)$$

2.7. Model 1: back trajectory modeling

We used SMF to concentrate SARS-CoV-2 RNA from the raw wastewater samples stored at 4 °C. The delay times in sample processing with SMF approach are provided in Table 1.

To approximate the initial concentration of SARS-CoV-2 gene fragments on the sampling day, a model was derived based on the previously reported decay rate constants for N1 (Ahmed et al., 2020b) and N2 (Hokajärvi et al., 2021a) genes at 4 °C in untreated wastewater (Table 2). The literature on the decay rates of SARS-CoV-2 RNA in wastewater at 4 °C is insufficient to determine a constant decay rate for different scenarios and geographies. Therefore, decay rates employed in this study serve as an uncertainty reference to approximate the initial concentration rather than a constant decay rate. Both Ahmed et al. (2020b) and Hokajärvi et al. (2021a) linearized the observed RNA concentrations using the natural logarithm (ln)-transformation of the normalized concentrations (Eq. 2). The decay rate (k) for N2 was re-calculated as 0.063 ($R^2 = 0.99$) in units per day by linear regression using the data reported by Hokajärvi et al. (2021a), while the decay rate (k) reported by Ahmed et al. (2020b) was used for N1 assay.

$$\mathrm{Ln}\left(\frac{C_t}{C_0}\right) = -k * t \tag{2}$$

where C_t is the concentration at time t, C_0 represents the initial concentration (estimated concentration), and k indicates the decay rate. A log-linear model was derived from Eq. 2 for the back-calculation of N1 and N2 concentrations (gene copies) as shown in Eq. 3, where C_t is the concentration of N1 or N2 genes at time t, C_0 is the initial concentration of N1 or N2 genes at the sampling day, k is the decay rate of N1 or N2 genes, and t is the delay in processing the samples.

$$C_0 = \frac{C_t}{e^{-k*t}} \tag{3}$$

2.8. Model 2: estimation of number of shedding cases, and SARS-CoV-2 concentration

The second model was adopted from Gerrity et al. (2021) with slight changes to estimate SARS-CoV-2 RNA concentration and number of shedding cases as a function of new cases in the city, fecal shedding rate, and daily total wastewater flowrate. The model was rewritten in RStudio since the original script was written in MATLAB. This model assumes the feces production rate for high-income countries and initial fecal shedding rate are 126 g/person-d (Rose et al., 2015) and $10^{8.9}$ GC/g feces with a decay rate $10^{0.35}$ GC/g feces-day, respectively (Gerrity et al., 2021; Wölfel et al., 2020). The ascertainment ratio was assumed as 2 (Gerrity et al., 2021), which means the model will multiply the number of cases by 2. Instead of assuming a constant daily wastewater flow rate, we used daily wastewater flow rates provided by the city of Winnipeg. Based on the shedding rate and shedding decay rate, an infected person is expected to shed SARS-CoV-2 for 26 days with a burst on the initial days of infection. The generated results were compared to the observed and back-calculated concentrations of SARS-CoV-2 RNA to justify back-calculations, and lead a discussion on predicting the actual number of active cases (Gerrity et al., 2021).

2.9. Epidemiological data

Information regarding new, cumulative and active cases, and test-positivity rates of COVID-19 for the whole population was provided by the Manitoba Regional Health Authority (Manitoba, 2021). Epidemiological data at the sub-catchment level was not available.

3. Results and discussion

3.1. Evaluation of SARS-CoV-2 concentration methods

Viral concentration with UF-3k ×*g* resulted in 13.38 ± 9.11% recovery (Fig. 1) and a final volume varying between 500 and 1200 mL. The high standard deviation could be attributed to the losses between the two-step ultrafiltration process. This two-step process resulted in high final volumes, which require multiple bead tubes and additional use of extraction kit solutions for RNA extraction since bead tubes have a maximum capacity of 300 μL of sample. During extraction, all tubes of the same sample were eluted into the same spinning column to collect total RNA. The use of multiple bead tubes can be another reason for the high variability in the recovery efficiency.

To decrease variability in recovery efficiency potentially caused by the use of multiple bead tubes, the centrifugation speed of Microsep Advance Centrifugal Device was increased from 3000*g* to 7500*g*, which generally resulted in a final volume less than 400 mL. The first trial with UF-7.5k ×*g* resulted in 4.79% recovery of Armored RNA (Fig. 1). After getting negative or weak SARS-CoV-2 genetic signals in wastewater samples with UF-7.5k ×*g*, further recovery experiments were conducted to determine recovery efficiency at 7500*g*, but Armored RNA was not recovered. Apparently, increasing the centrifugation speed impacted the recovery, probably caused Armored RNA to pass through or bind onto the filters. Filtration with cheesecloth and low-protein binding 0.45 and 0.2 μm 47-mm membrane filters before ultrafiltration might also be another reason for no detection and weak signals of SARS-CoV-2 RNA due to the elimination of solid particles, which could carry a significant amount of SARS-CoV-2 RNA (D'Aoust et al., 2021; Graham et al., 2021; Westhaus et al., 2021).

SMF was later employed to concentrate and detect SARS-CoV-2 RNA in wastewater samples. Using Armored RNA as a control, 15.27 ± 3.32% of recovery was achieved from the spiked wastewater samples (Fig. 1). SMF has the highest recovery efficiency with the smallest standard deviation, whereas UF-7.5k ×*g* has the lowest recovery efficiency with five negative samples out of six samples. This method did not employ a prefiltration step with cheesecloth and low-protein binding 0.45 and 0.2 μm 47-mm membrane filters. Therefore, the losses due to the elimination of solid particles were minimized and might have been reflected through the higher percentage and lower variation in recovery. Percent recovery values for SMF were comparable to the recovery values reported by Philo et al. (2021). They also reported 30% positivity rate for SARS-CoV-2 with SMF.

3.2. Detection of SARS-CoV-2 RNA in influent and effluent wastewater and primary sludge

3.2.1. Virus concentration method determines the detection of SARS-CoV-2 RNA in influent samples

Table 3 shows concentrations of SARS-CoV-2 RNA in wastewater and sludge samples collected during the sampling period. Three different concentration methods, namely UF-3k ×*g*, UF-7.5k ×*g* and SMF, were applied (Fig. 2). UF-3k ×*g* and UF-7.5k ×*g* methods required a prefiltration step

Table 2
Reported decay rate characteristics of the SARS-CoV-2 RNA in untreated wastewater at 4 °C.

Assay	Decay rate (k)	R^2	T_{50} (days)	T_{90} (days)	T_{99} (days)	Reference
N1	0.084 ± 0.013	0.79		27.8 ± 4.45		(Ahmed et al., 2020b)
N2	0.06 ± 0.0	0.99	11	36.00	73.00	(Hokajärvi et al., 2021a)

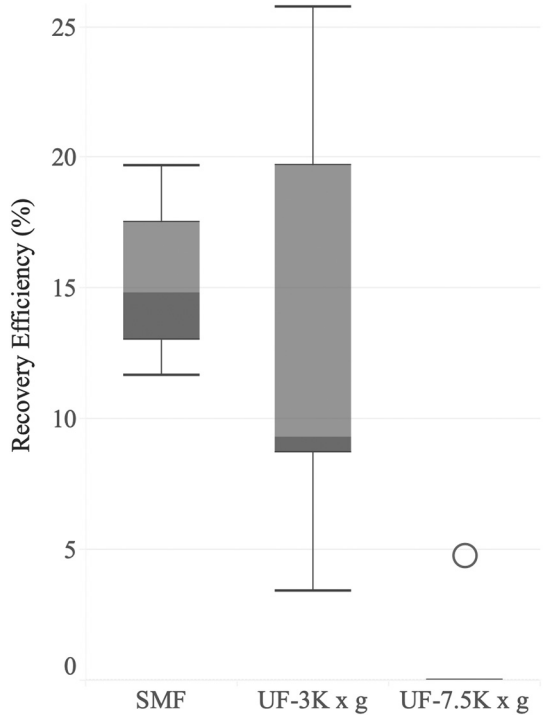

Fig. 1. Percent recovery and statistical analysis for each method.

with 0.45 and 0.2 μm filters to eliminate the effects of solids on ultrafiltration performance and separate viral fraction from bacterial fraction. On the other hand, SMF did not require any prefiltration step, and therefore SARS-CoV-2 RNA on solids was also concentrated with this method. All influent and effluent samples were processed using UF-3k $\times g$ method (Fig. 2). Influent samples collected between October 28th and December 15th were processed with both UF-3k $\times g$ and UF-7.5k $\times g$ methods. They were first concentrated with UF-7.5k $\times g$ method, and the negative samples were further processed with UF-3k $\times g$ method within 4 days of sampling. As samples were negative when processed with UF-3k $\times g$ and UF-7.5k $\times g$ methods between November 16th and December 15th (Fig. 2), SMF method was applied subsequently (Table 1) to concentrate SARS-CoV-2 from these samples stored at 4 °C. SARS-CoV-2 RNA was detected in all influent samples collected between September 30th and December 15th, except October 28th. SARS-CoV-2 RNA was detected only in influent samples collected from SESTP on October 28th.

Non-detection of SARS-CoV-2 RNA with UF-3k $\times g$ and UF-7.5k $\times g$ methods can be attributed to several factors, such as degradation during transportation and storage of samples (Ahmed et al., 2020b; Bivins et al., 2020a; Hokajärvi et al., 2021a; Hokajärvi et al., 2021b), losses during virus concentration (Chik et al., 2021; Ye et al., 2016), losses during extraction, and PCR related issues, such as inhibition and incomplete reverse transcription (Bustin et al., 2009). Since the variables in this study were the storage period at 4 °C and virus concentration methods, the storage period and the type of concentration method could explain the variations in detection with different concentration methods. SARS-CoV-2 RNA was detected with UF-3k $\times g$ method only on September 30th and October 14th (Fig. 2). All samples processed 4 days after collection were negative, possibly due to decay of SARS-CoV-2 RNA at 4 °C (Ahmed et al., 2020b; Hokajärvi et al., 2021a) and partitioning of SARS-CoV-2 to the solid phase rather than liquid phase (Chik et al., 2021). The time required for the decay of 90% (T_{90}) of N1 and N2 genes at 4 °C was reported as 27.8 ± 4.45 and 36 days by Ahmed et al. (2020b) and Hokajärvi et al. (2021a). Considering that T_{90} values being much greater than four days, the decay of SARS-CoV-2 RNA might not have lowered SARS-CoV-2 RNA concentration in influent samples to undetectable levels. Moreover, Markt et al. (2021) reported a minimal reduction in SARS-CoV-2 RNA concentrations in 9 days when stored at 4 °C. Therefore, attachment of SARS-CoV-2 to solids, concentration method, and variation in recovery efficiency are plausible causes for the non-detection of SARS-CoV-2 RNA.

Several studies have reported a higher affinity of enveloped viruses (mouse hepatitis virus [MHV] and *Pseudomonas* phage Φ6) to attach solid particles in wastewater compared to non-enveloped viruses (Ye et al., 2016), which might be the case for the non-detection of SARS-CoV-2 RNA in influent filtrates in this study. Attachment of SARS-CoV-2 to solids and variations in recovery efficiencies together possibly resulted in non-detection. This was further confirmed by the analysis of solid particles retained on the filters (Table 4). The difference of one order of magnitude between SARS-CoV-2 RNA concentrations in solids and filtrate indicated the significance of solid phase partitioning of SARS-CoV-2. For some samples, SARS-CoV-2 RNA concentration was even higher in solids. Higher detection frequency of SARS-CoV-2 N2 gene frequency in solids (89%) compared to that in the supernatant (67%) was also reported by Hokajärvi et al. (2021a). Furthermore, higher concentrations of SARS-CoV-2 RNA were observed in solids (Table 4) when total solids concentrations were higher in the samples collected from NESTP between October 28th and November 18th (Table S4). This increase can be attributed to

Table 3
Concentration of SARS-CoV-2 RNA in influents of three WWTPs. Influent samples collected between November 16th and December 15th (shown in a box) were late processed samples with SMF.

Sampling date	NESTP						SESTP						WESTP					
	Influent (GC/L)		Primary sludge (GC/mL)		Effluent (GC/L)		Influent (GC/L)		Primary sludge (GC/mL)		Effluent (GC/L)		Influent (GC/L)		Primary sludge (GC/mL)		Effluent (GC/L)	
	N1	N2	N1	N2	N1	N2	N1	N2	N1	N2	N1	N2	N1	N2	N1	N2	N1	N2
8-Jul	0	0	–	–	0	0	0	0	–	–	0	0	0	0	–	–	0	0
22-Jul	0	0	–	–	0	0	0	0	–	–	0	0	0	0	–	–	0	0
5-Aug	0	0	–	–	0	0	0	0	–	–	0	0	0	0	–	–	0	0
19-Aug	0	0	–	–	0	0	0	0	–	–	0	0	0	0	–	–	0	0
2-SeP	0	0	–	–	0	0	0	0	–	–	0	0	0	0	–	–	0	0
16-Sep	0	0	–	–	0	0	0	0	–	–	0	0	0	0	–	–	0	0
30-Sep	6087	25,713	–	–	0	0	8778	20,009	–	–	0	0	25,087	47,557	–	–	0	0
14-Oct	13,222	34,751	–	–	0	0	26,670	47,714	–	–	0	0	28,894	47,226	–	–	0	0
28-Oct	0	0	–	–	0	0	7544	21,084	–	–	0	0	0	0	–	–	0	0
12-Nov	3.3E+6	2.5E+6	7980	4960	–	–	1.2E+6	3.4E+6	3140	2740	–	–	9.6E+5	1.1E+6	2080	660	–	–
16-Nov	51,400	26,668	96,200	8860	–	–	12,964	17,410	2400	1360	–	–	16,506	4372	0	0	–	–
18-Nov	16,249	55,512	8540	6480	–	–	5843	17,412	3280	3040	–	–	13,762	11,844	0	380	–	–
1-Dec	20,980	16,833	7480	6740	–	–	11,261	6780	3100	2260	–	–	5519	2214	0	260	–	–
8-Dec	15,722	11,463	12,580	5860	–	–	4984	9685	7560	2760	–	–	9007	5300	820	180	–	–
15-Dec	20,371	13,120	3220	1400	–	–	17,209	8188	3020	740	–	–	5535	5211	5660	2600	–	–

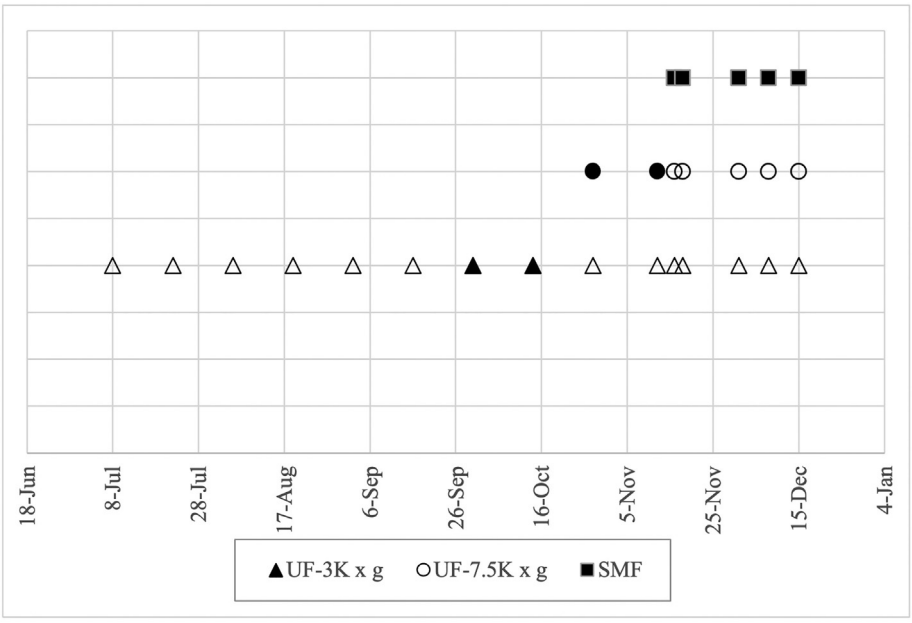

Fig. 2. Detection of SARS-CoV-2 RNA in influent samples with different concentration methods. Filled shapes represent the samples that are SARS-CoV-2 RNA positive, i.e. C_T is <40.

the increase in total solids, which might result in elevated levels of the partitioning of SARS-CoV-2 to solid phase. The relationship between case data (Fig. 3) and SARS-CoV-2 RNA concentration in solids during this period should not be overlooked, as discussed in Section 3.2.4. Similarly, some other studies also emphasized solids-associated behavior of SARS-CoV-2 by taking the absorption of viral particles to solids into consideration and reporting the correlations between virus concentration and case data (D'Aoust et al., 2021; Graham et al., 2021; Peccia et al., 2020).

Effects of freezing and thawing on SARS-CoV-2 RNA concentrations in solids should also be considered in this study. We extracted SARS-CoV-2 RNA from solids on filters stored at −20 °C that were later subjected to freeze-thaw once. Markt et al. (2021) reported a significant SARS-CoV-2 RNA reduction in influent samples subjected to one freeze-thaw cycle. In comparison with these results, Simpson et al. (2021) and Hokajärvi et al. (2021a) observed a relatively lower reduction of SARS-CoV-2 RNA in solids after one cycle of freeze-thaw, but still up to 60% of reduction. Considering current literature, the actual SARS-CoV-2 RNA concentrations in solids might be higher than the measured concentrations. Moreover, the presence of solids in wastewater might enhance the stability of SARS-CoV-2 RNA (Kitajima et al., 2020).

Since SARS-CoV-2 is predominantly in contact with fecal matter in the wastewater matrix during the transportation to the WWTPs via sewer systems, recovery efficiency determination approaches, which are generally based on a spike-and-recovery approach, might not sufficiently reflect the actual recovery values of SARS-CoV-2 RNA (Chik et al., 2021). This could be due to several reasons in the current study. First, there were only 30 min between sample spiking and processing in this study. Secondly, physicochemical characteristics of the spiked wastewater samples could be significantly different from influent samples that were processed in this study. Amoah et al. (2022) previously demonstrated the effects of pH, ammonia, and total solids on detection and SARS-CoV-2 RNA concentration. Thus, the actual recovery of SARS-CoV-2 RNA might be much lower than the assessed recovery efficiencies for UF-3k ×g and UF-7.5k ×g considering spike-and-recovery approaches and variations in physicochemical characteristics of the samples.

SARS-CoV-2 RNA was detected in the samples using SMF (Fig. 2 and Table 3), although the sample processing was delayed between 46 and 75 days (Fig. 2). The successful detection of the virus was most probably because of the inclusion of both solids and supernatant into sample processing with SMF. An inter-laboratory study processing wastewater samples collected on the same day from a WWTP in Winnipeg also reported that SARS-CoV-2 RNA was detected only by the laboratories processing samples with the methods focusing on solids (Chik et al., 2021). Another study on the partitioning of enveloped viruses to wastewater solids strengthens the claim of such solid-associated behavior with concentrations of enveloped viruses in solids found 1000 times higher than those in influent on a per mass basis (Ye et al., 2016). As a matter of fact, many other studies have suggested that a wastewater solids-based measurement of SARS-CoV-2 RNA might be a more sensitive approach than a wastewater supernatant-based one (D'Aoust et al., 2021; Graham et al., 2021; Peccia et al., 2020; Westhaus et al., 2021). Moreover, input volumes of SMF (500 mL), UF-3k ×*g* (120 mL) and UF-7.5k ×*g* (120 mL) might be another factor determining detection of SARS-CoV-2 RNA especially when the virus is not abundant in the samples. Although the studies on the stability and detection of SARS-CoV-2 RNA in influent and solids are limited, the current findings point out the predominant partitioning of SARS-CoV-2 to solid phase and higher stability of SARS-CoV-2 RNA in solids. The results of this study, together with previous studies (Chik et al., 2021; Hokajärvi et al., 2021a; Markt et al., 2021), underscores the importance of the inclusion of both solids and supernatant fractions in wastewater processing for the detection of SARS-CoV-2 RNA. However, adsorption capacity of SARS-CoV-2 to wastewater solids needs to be investigated under different environmental conditions.

Table 4
SARS-CoV-2 RNA concentration in influent solids from NESTP, SESTP and WESTP.

Date	NESTP		SESTP		WESTP	
	N1 (GC/L)	N2 (GC/L)	N1 (GC/L)	N2 (GC/L)	N1 (GC/L)	N2 (GC/L)
2-Sep	0	0	0	0	0	0
16-Sep	0	0	0	0	0	0
30-Sep	–	–	232,059	367,283	75,185	0
14-Oct	75,422	0	76,814	0	0	0
12-Nov	335,397	516,635	149,704	95,908	49,617	78,529
16-Nov	302,821	113,570	0	26,192	159,752	29,619
18-Nov	626,217	242,533	128,595	42,033	307,246	147,921
1-Dec	43,106	26,877	69,835	49,772	120,428	60,634
8-Dec	45,194	21,513	31,191	14,206	15,026	12,649
15-Dec	–	–	–	–	–	–

3.2.2. Detection in primary sludge samples

Both N1 and N2 genomic targets of SARS-CoV-2 were detected in all primary sludge samples collected from NESTP and SESTP while they were not

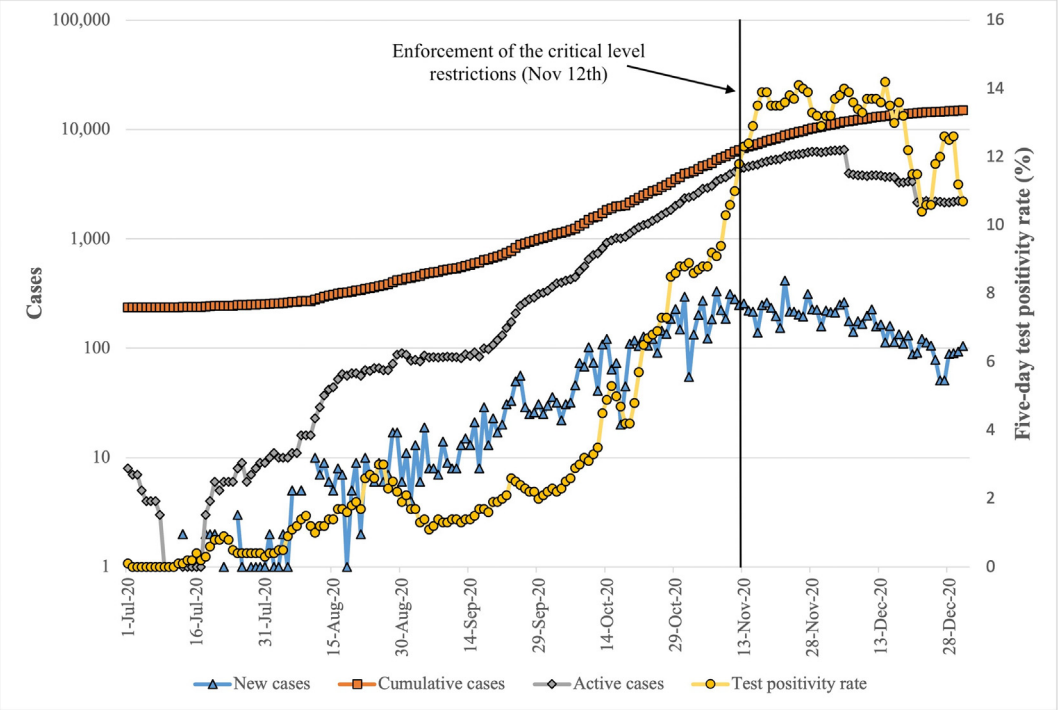

Fig. 3. COVID-19 infection dynamics in Winnipeg. Temporal changes in the numbers of new, active, and cumulative cases and five-day test positivity rate during sampling period.

detected on November 16th, and only N2 was detected on November 18th and December 1st in the samples collected from WESTP (Table 3). The input volume of primary sludge samples processed for the detection of SARS-CoV-2 RNA in this study was only 300 μL, which is much lower than the input volumes in previous studies (Graham et al., 2021; Peccia et al., 2020). Still SARS-CoV-2 RNA was detected, indicating the high density of SARS-CoV-2 RNA in primary sludge.

Detection of SARS-CoV-2 RNA in primary sludge samples could be associated with the input volume and total solids. Low input volumes can cause biases in the detection and quantification of SARS-CoV-2 RNA when virus concentration in the sample is low, and the samples are not homogenous in terms of total solids and SARS-CoV-2 RNA distribution. Considering the high affinity of enveloped viruses to attach to the solids particles (Ye et al., 2016), total solids concentration can be another determinant of detection and quantification of SARS-CoV-2 RNA in primary solids in addition to the community infection dynamics. In fact, concentration of SARS-CoV-2 RNA was generally the highest in the samples collected from NESTP with an average primary sludge density of 3.53 ± 0.84% and was generally the lowest in the samples collected from WESTP with an average sludge density of 0.37 ± 0.06% (Table S5). This statement assumes homogeneous distribution of prevalence and incidence throughout the city of Winnipeg on the sampling days based on the high correlation between influent viral concentrations in WWTPs ($r > 0.91$ for N1 and $r > 0.72$ for N2) (Table S6). Higher input volumes should be considered for consistent and sensitive detection and quantification of the viral RNA in sludge samples.

3.2.3. Detection in effluent samples

SARS-CoV-2 RNA was not detected in both secondary and final effluent samples of all three WWTPs (Table 3), although it is worth mentioning that WESTP employs solar disinfection, which effectively reduces bacteria and is questionable in removing viruses, especially in cold climate conditions (Parsa et al., 2021). Employing UV disinfection, NESTP and SESTP might have effectively reduced SARS-CoV-2 RNA concentration below detectable levels in final effluent. SARS-CoV-2, being an enveloped virus, is expected to be more sensitive to disinfection processes (UV, ozonation, and chlorination) than non-enveloped viruses (Chen et al., 2021; Saawarn and Hait, 2021). Non-detection of SARS-CoV-2 RNA in tertiary-treated effluent samples was also reported elsewhere (Randazzo et al., 2020; Sherchan et al., 2020), indicating the efficacy of disinfection processes in the removal of SARS-CoV-2 RNA considering high positivity rates (>83%) in influent samples. This claim was further supported by the occurrence of SARS-CoV-2 RNA in secondary-treated effluent (before disinfection) samples (Haramoto et al., 2020; Randazzo et al., 2020).

SARS-CoV-2 RNA is removed not only by disinfection processes but also primary and secondary treatment processes, which can also effectively reduce SARS-CoV-2 concentration in the WWTPs (Balboa et al., 2021; Randazzo et al., 2020; Sherchan et al., 2020). Detection of SARS-CoV-2 RNA in very low volumes of primary sludge samples in this study might indicate a significant removal of SARS-CoV-2 RNA with primary treatment. While removal of SARS-CoV-2 RNA with primary, secondary and tertiary treatments could explain non-detection of SARS-CoV-2 RNA in effluent samples to a great extent, elimination of solid particles with prefiltration of effluent samples with 0.45 and 0.2 μm filters and concentrations of SARS-CoV-2 RNA at non-detectable levels could be other factors considering the attachment of SARS-CoV-2 to solids. However, more studies are needed to fully uncover the fate of SARS-CoV-2 in WWTPs and the effects of virus concentration methods and input volume on the detection and quantification of SARS-CoV-2 RNA in effluent samples.

Several studies have reported that SARS-CoV-2 RNA can be found in wastewater and watershed impacted by wastewater discharge in different states: free RNA, non-infectious but protected genome and infectious particles at different proportions (Bivins et al., 2020a; Wang et al., 2021; Wurtzer et al., 2021). Quantitative microbial risk assessment studies have shown that transmission risks are likely to exceed tolerable infection risk for SARS-CoV-2 for aggressive and extreme scenarios (Dada and Gyawali, 2021; Zaneti et al., 2021). These findings suggest wastewater systems as a potential transmission route of SARS-CoV-2 considering the proportion of infectious particles in wastewater. Therefore, the study of the fate of SARS-CoV-2 RNA in wastewater treatment systems remains significant and validates the need for further elucidation. In Winnipeg, the proportion of reported active cases to the total population in the city was about 1% at its highest, which is well above the level of moderate scenarios and may

infer a possible occupational health risk in wastewater, especially during the first stages of wastewater treatment (screening, grit removal, primary treatment, and primary sludge handling).

3.2.4. Detection of SARS-CoV-2 RNA relates to the number of cases and test positivity rate

SARS-CoV-2 RNA was first detected at a concentration of <50 gene copies per milliliter (GC/mL) on September 30th in all influent wastewater samples collected from NESTP, SESTP, and WESTP (Table 3) when the number of the reported new cases and active cases in Winnipeg were 25 and 321, respectively (Fig. 3). This first detection concentration on September 30th went up to 400 GC/mL after the concentration of the viral RNA in the solids was added to the concentration in supernatant. Detection of SARS-CoV-2 RNA in wastewater samples collected from a WWTP in Winnipeg on August 31st was first reported by Chik et al. (2021) at trace concentrations (<20 GC/mL), with the concentration methods focusing on solid fraction when the number of the reported new and active cases were 11 and 85, respectively. Both results suggest a larger number of new and active cases consisting of asymptomatic, presymptomatic, and recovering cases of COVID-19 in the community. This is consistent with the estimations of the actual number of infections being 3 to 20 (Wu et al., 2020) and 6 to 24 times (Havers et al., 2020) higher than reported cases in the U.S. A study by Hong et al. (2021) focusing on the estimation of the minimum number of SARS-CoV-2 infected cases for the detection of viral RNA in wastewater estimated a minimum number of active cases of 253 to 459 positive cases per 10,000 population to detect SARS-CoV-2 RNA in wastewater, which is much higher than the number of active cases on the day of the first detection in Winnipeg considering the population of Winnipeg (766,900) (Winnipeg, 2021). However, the reported range of active cases needed for the detection of SARS-CoV-2 RNA might be a system- or site-specific estimation since the detection of SARS-CoV-2 RNA in wastewater depends on many factors, including sampling frequencies, concentration methods, and their recovery efficiencies, RT-qPCR detection performance, sample size, daily wastewater flow rates (dilution factor), and environmental factors which can affect the persistence and abundance of SARS-CoV-2 RNA in wastewater (Hong et al., 2021). Moreover, new cases predominantly contribute to the concentration of SARS-CoV-2 RNA in wastewater rather than active cases (Gerrity et al., 2021; Wu et al., 2022) due to higher viral shedding rates in the very early stages of the infection (Benefield et al., 2020; He et al., 2020; Wei et al., 2020; Wölfel et al., 2020). Therefore, the number of active cases, without the data for new and early-stage cases, may not be enough in determining the minimum number of cases to detect SARS-CoV-2 RNA in wastewater.

The difference between symptom onset and test confirmation suggests that time-lag might be another explanation for the detection of SARS-CoV-2 RNA when the number of active cases was low. There is also a typical 4-to-5-day incubation period before onset of the symptoms (He et al., 2020; Li et al., 2020). A possible effect of time-lag can be further confirmed by the sharp increase in the number of cases and five-day test positivity rate (Fig. 3) after September 30th. Between the first sampling date, July 8th, and September 30th, the five-day test positivity rate fluctuated between 0.0% and 3.0% (Fig. 3) (Manitoba, 2021). On September 30th, the test positivity rate was 2.1%, and subsequently, a constant increase in the test positivity rate until mid-December was recorded, with a peak test positivity rate of 14.2% on December 14th. During this period, we detected SARS-CoV-2 RNA in all influent samples (including solids fractions) collected from three wastewater treatment plants, except on October 28th (Table 3), using different concentration methods.

Previous studies have reported associations between the concentration of SARS-CoV-2 RNA in primary settled solids and COVID-19 cases (Graham et al., 2021; Peccia et al., 2020). In this study, SARS-CoV-2 RNA was detected in almost all primary sludge samples. In the previous sections, the fluctuations in the concentration of SARS-CoV-2 RNA were partly associated with total solids in the samples. A direct correlation between concentrations and reported cases is intentionally avoided due to low-resolution sample collection and small input volumes of primary sludge. These two factors cause some difficulties in justifying the fluctuations in SARS-CoV-2 RNA concentrations in primary sludge samples. In other words, it is not clear if solids, the number of infections, or a combination of them cause fluctuations in SARS-CoV-2 RNA concentrations. High-resolution sample collection (at least weekly) and larger input volumes could generate more reliable and consistent results for a wastewater surveillance study.

3.3. Estimation of concentrations and shedding cases

Using reported decay rates for N1 and N2 gene fragments (Ahmed et al., 2020b; Hokajärvi et al., 2021a), initial concentrations of SARS-CoV-2 RNA in the late-processed influent samples, collected between November 16th and December 15th, were estimated and then converted into normalized concentration using Eq. 1. Reported COVID-19 infection dynamics and observed and estimated concentrations were compared with infection dynamics and modeled concentrations generated by model 2 as an attempt to justify models and understand the course of COVID-19 infection dynamics in the city. Lack of information regarding population and COVID-19 infection dynamics in each sewershed is one of the limitations of this study, preventing us from doing a sewershed-based analysis.

Peak concentrations of SARS-CoV-2 RNA were measured on the day when critical-level restrictions were enforced. Estimated concentrations were the highest on the following 4th and 6th days (Fig. 4). Observed concentrations from September 30th to November 12th and estimated concentrations were generally in close proximity with the modeled concentrations for at least one genomic target. Estimated concentrations, calculated based on observed concentrations of late-processed samples using Eq. 3, were treated as observed concentrations to interpret the relationship between concentration of SARS-CoV-2 RNA and infection dynamics. Different decay rates for N1 and N2 resulted in higher estimated concentrations of N1 for late-processed samples, while the difference between N1 and N2 concentrations for the rest of the samples was smaller than 0.35 on $\log_{10}$ scale (Fig. 4). The decay rate of N1 was calculated based on the degradation of genomic signals of gamma-irradiated SARS-CoV-2 by Ahmed et al. (2020b) and had a higher standard deviation of 15% and lower R^2 of 0.79 compared to those values of N2, which were based on the degradation of active SARS-CoV-2 (Hokajärvi et al., 2021a) (Table 2). Gamma irradiation of SARS-CoV-2 and relatively higher variations in the decay rate of N1 might result in significant biases in such a back-trajectory modeling approach for N1. Additionally, the decay rate of N2 was determined in Finland, climate and socioeconomic status of which is comparable with Canada. Therefore, we mostly consider N2 concentrations for back-trajectory modeled samples in the discussion.

The critical level restrictions in Manitoba were applied when extensive community transmission of COVID-19 occurred, outbreaks could not be controlled, and a heavy toll on the healthcare system was expected. With the enforcement of the restrictions on November 12th, gatherings and travels were extremely restricted, and schools and non-essential businesses were closed. Bearing in mind that the outbreak and transmission are at the critical levels when the restrictions are applied, the occurrence of a much higher number of new cases compared to reported numbers is most likely because of the limited testing capacity at the peak times and time-lag between the incubation period of SARS-CoV-2, onset of the symptoms and test confirmation (He et al., 2020; Li et al., 2020). In this study, such a scenario was validated with the concentrations of SARS-CoV-2 RNA in influent that peaked following the enforcement in November and significantly lowered to the modeled concentrations in December as the outbreak was contained. The difference between the concentrations of N2 and modeled concentrations (0.79 to 0.97 on $\log_{10}$ basis) in November suggests that the actual number of cases might be much higher than reported numbers, which is further supported by the sharp increase in test-positivity rates and the number of new cases (Fig. 3). These findings correspond to the findings of Havers et al. (2020), reporting that the actual number of cases can be as high as 24 times of reported numbers.

In general, observed (September 30th to November 12th) and estimated (November 16th to December 15th) concentrations were sensitive to the

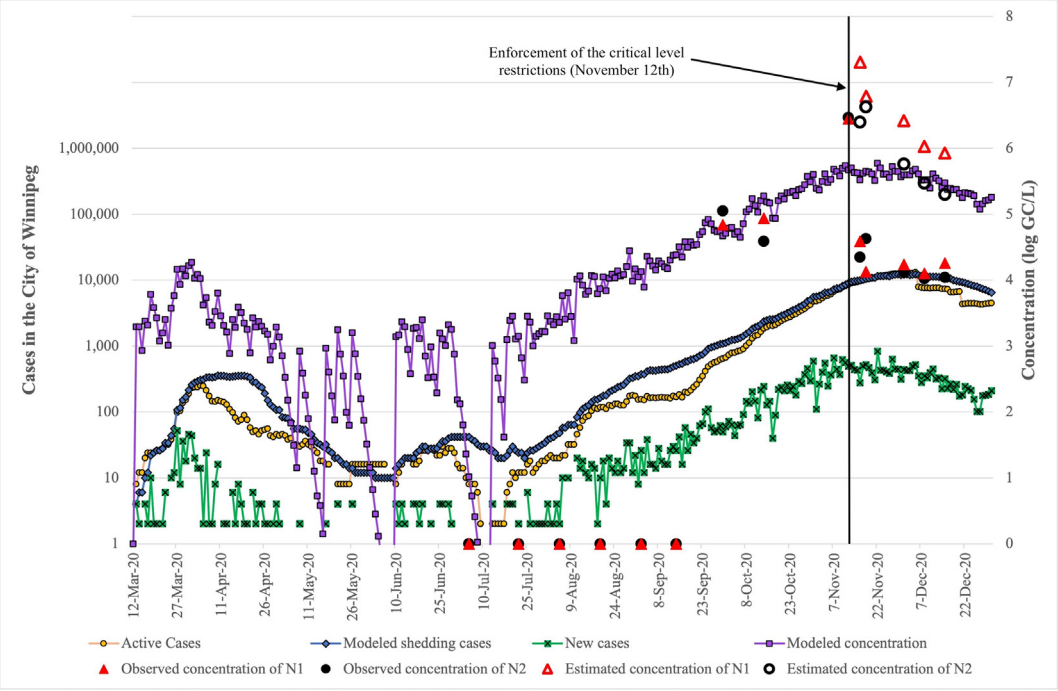

Fig. 4. Modeled (purple squares), observed (filled red triangles and black circles) and estimated (red triangles and black circles) concentrations of SARS-CoV-2 RNA as log10 concentrations and COVID-19 infection dynamics from the beginning of the outbreak in Winnipeg. Observed concentrations between September 30th and November 12th are the sum of the concentration in solids and filtrates since the latter concentrations were obtained using SMF which concentrates viruses from both supernatant and solids. Estimated concentrations between November 16th and December 15th are calculated using Eq. 3. Observed concentrations are represented for both N1 (filled red triangles) and N2 (filled black circles). Green x represents new cases in Winnipeg corrected with an ascertainment ratio of 2. Oranges circles represent active cases in Winnipeg corrected with an ascertainment ratio of 2. Blue diamonds represent modeled shedding cases in Winnipeg, i.e. modeled active cases. (For interpretation of the references to color in this figure legend, the reader is referred to the web version of this article.)

fluctuations in test-positivity rates and the number of new cases except for the samples collected in November. Model 2 assumed an ascertainment ratio of 2, which is an optimistic assumption considering ascertainment ratios up to 24 in the literature (Havers et al., 2020; Wu et al., 2020). While an ascertainment ratio of 2 in the model generated comparable concentrations with the concentrations for September, October, and December samples, a higher ascertainment ratio might come into question during the peak times in November. The high concentrations and ascertainment ratios in November can be explained by the high transmission rates of the disease and the number of asymptomatic and presymptomatic cases around this period. After the enforcement of critical level restrictions, public mobility and disease transmission were expected to be minimized. However, the number of new cases and the test-positivity rate remained high during the sampling in November and December, most likely due to time-lag associated with the peaking of viral load and disease transmissivity prior to symptom onset (Benefield et al., 2020; He et al., 2020; Wei et al., 2020). Probably most individuals were infected around the first day of the enforcement but developed symptoms later, which was in agreement with the typical incubation period of 4–5 days before symptom onset (Guan et al., 2020; Lauer et al., 2020; Li et al., 2020), and only sought healthcare and underwent testing after symptom onset. SARS-CoV-2 RNA load in December might be due to prolonged shedding from individuals infected earlier. Additionally, individuals infected before the enforcement can infect other people living with them in subsequent days, and disease transmission can still be high among essential workers and their families after the enforcement.

Estimation of SARS-CoV-2 RNA concentration based on shedding rate and reported cases has been previously studied with an emphasis on the significant contribution of newly infected individuals to SARS-CoV-2 RNA loads in wastewater and occurrence of the highest fecal shedding rates in the first days of infection before symptoms develops and tests are conducted (Gerrity et al., 2021; Wu et al., 2022). They also reported high similarity between the observed and modeled concentrations, which validates the efficacy of such models to estimate concentration and infection dynamics. Sensitivity of SARS-CoV-2 RNA levels in wastewater to the fluctuations in the number of new cases and test-positivity rates in this study suggest that an initial burst of viral shedding may occur in the very early stages of COVID-19 infection even before symptom onset and may be followed by a prolonged period of lower shedding rates up to 30 days as reported by Chen et al. (2020), Hoffmann and Alsing (2021), Wölfel et al. (2020) and Wu et al. (2022).

Our data suggest that a back-trajectory model as a function of decay rate and time may be used to estimate initial concentrations of late-processed samples as it fit the modeled concentrations and fluctuations in new cases. High-resolution sampling and site-specific decay rates may help to validate and improve the model. Time-lag, testing capacity, and test-positivity rates in addition to the reported cases and shedding rate should also be considered for the shedding rate-based models to obtain better model fits and estimations.

4. Conclusions

Wastewater surveillance of COVID-19 has been considered as an early-warning tool for potential outbreaks and an informative method to characterize COVID-19 infection dynamics. However, researchers have not reached a consensus on sample collection and processing, and data analysis. Furthermore, the potential discharge of SARS-CoV-2 from wastewater treatment plants to the environment is another issue that requires a comprehensive investigation of the fate of SARS-CoV-2 throughout the wastewater treatment process.

The current study focused on the detection of SARS-CoV-2 RNA in wastewater and sludge samples and the relationship between detection and infection dynamics in Winnipeg. Our results showed that SARS-CoV-2 RNA might predominate in solids. Concentration methods focusing on both supernatant and solids fractions may perform better in virus recovery,

especially for enveloped viruses. Thus, the type of concentration method may significantly affect SARS-CoV-2 RNA recovery from influent samples.

SARS-CoV-2 RNA might be substantially removed during primary and secondary treatment as SARS-CoV-2 RNA was detected in influent and primary sludge but not in secondary and final effluents. The high affinity of SARS-CoV-2 to solids and detection of SARS-CoV-2 RNA in primary sludge samples at high concentrations suggest sludge line as a potential removal mechanism and a sampling spot for wastewater surveillance. Improvement in processing sludge samples for viral concentration and detection is required to gain more insight into the fate of SARS-CoV-2 RNA in sludge line.

In addition to the detection and fate of SARS-CoV-2 RNA in WWTPs, the proposed study underlines the relationship between SARS-CoV-2 RNA levels in influent samples and infection dynamics characterized by increasing COVID-19 incidence and prevalence during the sampling period. Observed, estimated and modeled concentrations were sensitive to the fluctuations in new cases and test-positivity rates, suggesting an early burst of viral shedding in infected individuals. During the peak times, the number of infections can be much higher than the number of reported cases considering the time-lag between infection and test confirmation, and asymptomatic infections. To confirm our findings and improve such shedding rate-based models, additional studies with higher sampling resolution and the models informed by other factors, such as time-lag, test capacity, and test-positivity rates, are required. Overall, this study demonstrates that SARS-CoV-2 RNA may predominate in solids, and wastewater surveillance of COVID-19 can provide valuable insights into infection dynamics prior to clinical test confirmations.

CRediT authorship contribution statement

Kadir Yanaç: Conceptualization, Methodology, Validation, Formal analysis, Investigation, Data curation, Writing – original draft, Visualization, Project administration. **Adeola Adegoke:** Software, Formal analysis. **Liqun Wang:** Software, Formal analysis. **Miguel Uyaguari:** Conceptualization, Methodology, Validation, Resources, Writing – review & editing, Supervision, Project administration, Funding acquisition. **Qiuyan Yuan:** Conceptualization, Methodology, Validation, Resources, Writing – review & editing, Supervision, Project administration, Funding acquisition.

Declaration of competing interest

There are no conflicts of interest to declare.

Acknowledgments

This work was supported by NSERC Alliance Covid-19 Grant (Grant No. 431401363, 2020–2021). We thank the City of Winnipeg, the management, and operators at the NESTP, SESTP, and WESTP for collecting samples and providing information regarding wastewater characteristics, in particular Jong Hwang, Brendan Hellrung, Mark Lefko, Jorge Martins, and Shaun Walker. We acknowledge Ms. Shana Mann and Miss Jocelyn Zambrano (University of Manitoba) for nucleic acid extraction from solids. We also thank Tri Le (University of Manitoba) for proofreading.

Appendix A. Supplementary data

Supplementary data to this article can be found online at https://doi.org/10.1016/j.scitotenv.2022.153906.

References

Ahmed, W., Angel, N., Edson, J., Bibby, K., Bivins, A., O'Brien, J.W., Choi, P.M., Kitajima, M., Simpson, S.L., Li, J., Tscharke, B., Verhagen, R., Smith, W.J.M., Zaugg, J., Dierens, L., Hugenholtz, P., Thomas, K.V., Mueller, J.F., 2020a. First confirmed detection of SARS-CoV-2 in untreated wastewater in Australia: a proof of concept for the wastewater surveillance of COVID-19 in the community. Sci. Total Environ. 728, 138764.

Ahmed, W., Bertsch, P.M., Bibby, K., Haramoto, E., Hewitt, J., Huygens, F., Gyawali, P., Korajkic, A., Riddell, S., Sherchan, S.P., Simpson, S.L., Sirikanchana, K., Symonds, E.M., Verhagen, R., Vasan, S.S., Kitajima, M., Bivins, A., 2020b. Decay of SARS-CoV-2 and surrogate murine hepatitis virus RNA in untreated wastewater to inform application in wastewater-based epidemiology. Environ. Res. 191, 110092.

Ahmed, W., Bertsch, P.M., Bivins, A., Bibby, K., Farkas, K., Gathercole, A., Haramoto, E., Gyawali, P., Korajkic, A., McMinn, B.R., Mueller, J.F., Simpson, S.L., Smith, W.J.M., Symonds, E.M., Thomas, K.V., Verhagen, R., Kitajima, M., 2020c. Comparison of virus concentration methods for the RT-qPCR-based recovery of murine hepatitis virus, a surrogate for SARS-CoV-2 from untreated wastewater. Sci. Total Environ. 739, 139960.

Alygizakis, N., Markou, A.N., Rousis, N.I., Galani, A., Avgeris, M., Adamopoulos, P.G., Scorilas, A., Lianidou, E.S., Paraskevis, D., Tsiodras, S., Tsakris, A., Dimopoulos, M.-A., Thomaidis, N.S., 2021. Analytical methodologies for the detection of SARS-CoV-2 in wastewater: protocols and future perspectives. TrAC Trends Anal. Chem. 134, 116125.

Amoah, I.D., Abunama, T., Awolusi, O.O., Pillay, L., Pillay, K., Kumari, S., Bux, F., 2022. Effect of selected wastewater characteristics on estimation of SARS-CoV-2 viral load in wastewater. Environ. Res. 203, 111877.

Balboa, S., Mauricio-Iglesias, M., Rodriguez, S., Martínez-Lamas, L., Vasallo, F.J., Regueiro, B., Lema, J.M., 2021. The fate of SARS-CoV-2 in WWTPs points out the sludge line as a suitable spot for detection of COVID-19. Sci. Total Environ. 772 (145268), 138764–138771. https://doi.org/10.1016/j.scitotenv.2021.145268.

Barril, P.A., Pianciola, L.A., Mazzeo, M., Ousset, M.J., Jaureguiberry, M.V., Alessandrello, M., Sánchez, G., Oteiza, J.M., 2021. Evaluation of viral concentration methods for SARS-CoV-2 recovery from wastewaters. Sci Total Environ 756 144105-144105.

Benefield, A.E., Skrip, L.A., Clement, A., Althouse, R.A., Chang, S., Althouse, B.M., 2020. SARS-CoV-2 viral load peaks prior to symptom onset: a systematic review and individual-pooled analysis of coronavirus viral load from 66 studies. medRxiv 2020.2009.2028.20202028.

Bi, Q., Lessler, J., Eckerle, I., Lauer, S.A., Kaiser, L., Vuilleumier, N., Cummings, D.A.T., Flahault, A., Petrovic, D., Guessous, I., Stringhini, S., Azman, A.S., 2021. Household transmission of SARS-CoV-2: insights from a population-based serological survey. Nat. Commun. 12 (1), 3643–3650. https://doi.org/10.1038/s41467-021-23733-5.

Bishop, N., Jones-Lepp, T., Margetts, M., Sykes, J., Alvarez, D., Keil, D.E., 2020. Wastewater-based epidemiology pilot study to examine drug use in the Western United States. Sci. Total Environ. 745 140697-140697.

Bisseux, M., Colombet, J., Mirand, A., Roque-Afonso, A.M., Abravanel, F., Izopet, J., Archimbaud, C., Peigue-Lafeuille, H., Debroas, D., Bailly, J.L., Henquell, C., 2018. Monitoring human enteric viruses in wastewater and relevance to infections encountered in the clinical setting: a one-year experiment in Central France, 2014 to 2015. Euro Surveill. 23 (7).

Bivins, A., Greaves, J., Fischer, R., Yinda, K.C., Ahmed, W., Kitajima, M., Munster, V.J., Bibby, K., 2020a. Persistence of SARS-CoV-2 in water and wastewater. Environ. Sci. Technol. Lett. 7 (12), 937–942.

Bivins, A., North, D., Ahmad, A., Ahmed, W., Alm, E., Been, F., Bhattacharya, P., Bijlsma, L., Boehm, A.B., Brown, J., Buttiglieri, G., Calabro, V., Carducci, A., Castiglioni, S., Cetecioglu Gurol, Z., Chakraborty, S., Costa, F., Curcio, S., de los Reyes, F.L., Delgado Vela, J., Farkas, K., Fernandez-Casi, X., Gerba, C., Gerrity, D., Girones, R., Gonzalez, R., Haramoto, E., Harris, A., Holden, P.A., Islam, M.T., Jones, D.L., Kasprzyk-Hordern, B., Kitajima, M., Kotlarz, N., Kumar, M., Kuroda, K., La Rosa, G., Malpei, F., Mautus, M., McLellan, S.L., Medema, G., Meschke, J.S., Mueller, J., Newton, R.J., Nilsson, D., Noble, R.T., van Nuijs, A., Peccia, J., Perkins, T.A., Pickering, A.J., Rose, J., Sanchez, G., Smith, A., Stadler, L., Stauber, C., Thomas, K., van der Voorn, T., Wigginton, K., Zhu, K., Bibby, K., 2020. Wastewater-based epidemiology: global collaborative to maximize contributions in the fight against COVID-19. Environmental Science & Technology 54 (13), 7754–7757.

Bustin, S.A., Benes, V., Garson, J.A., Hellemans, J., Huggett, J., Kubista, M., Mueller, R., Nolan, T., Pfaffl, M.W., Shipley, G.L., Vandesompele, J., Wittwer, C.T., 2009. The MIQE guidelines: minimum information for publication of quantitative real-time PCR experiments. Clin. Chem. 55 (4), 611–622.

Calgua, B., Mengewein, A., Grunert, A., Bofill-Mas, S., Clemente-Casares, P., Hundesa, A., Wyn-Jones, A.P., López-Pila, J.M., Girones, R., 2008. Development and application of a one-step low cost procedure to concentrate viruses from seawater samples. J. Virol. Methods 153 (2), 79–83.

Carducci, A., Federigi, I., Liu, D., Thompson, J.R., Verani, M., 2020. Making waves: coronavirus detection, presence and persistence in the water environment: state of the art and knowledge needs for public health. Water Res. 179, 115907.

CDC, 2020. 2019-Novel Coronavirus (2019-nCoV) Real-time rRT-PCR Panel Primers and Probes.

Chen, C., Hayward, K., Khan, S.J., Örmeci, B., Pillay, S., Rose, J.B., Thanikal, J.V., Zhang, T., 2021. Role of wastewater treatment in COVID-19 control. Water Qual. Res. J. Can. 56 (2), 68–82.

Chen, Y., Chen, L., Deng, Q., Zhang, G., Wu, K., Ni, L., Yang, Y., Liu, B., Wang, W., Wei, C., Yang, J., Ye, G., Cheng, Z., 2020. The presence of SARS-CoV-2 RNA in the feces of COVID-19 patients. J. Med. Virol. 92 (7), 833–840.

Chik, A.H.S., Glier, M.B., Servos, M., Mangat, C.S., Pang, X.-L., Qiu, Y., D'Aoust, P.M., Burnet, J.-B., Delatolla, R., Dorner, S., Geng, Q., Giesy, J.P., McKay, R.M., Mulvey, M.R., Prystajecky, N., Srikanthan, N., Xie, Y., Conant, B., Hrudey, S.E., 2021. Comparison of approaches to quantify SARS-CoV-2 in wastewater using RT-qPCR: results and implications from a collaborative inter-laboratory study in Canada. J. Environ. Sci. 107, 218–229.

D'Aoust, P.M., Mercier, E., Montpetit, D., Jia, J.J., Alexandrov, I., Neault, N., Baig, A.T., Mayne, J., Zhang, X., Alain, T., Langlois, M.A., Servos, M.R., MacKenzie, M., Figeys, D., MacKenzie, A.E., Graber, T.E., Delatolla, R., 2021. Quantitative analysis of SARS-CoV-2 RNA from wastewater solids in communities with low COVID-19 incidence and prevalence. Water Res. 188, 116560.

Dada, A.C., Gyawali, P., 2021. Quantitative microbial risk assessment (QMRA) of occupational exposure to SARS-CoV-2 in wastewater treatment plants. Sci. Total Environ. 763, 142989.

Day, M., 2020. Covid-19: identifying and isolating asymptomatic people helped eliminate virus in italian village. BMJ 368, m1165.

Diemert, S., Yan, T., 2020. Municipal wastewater surveillance revealed a high community disease burden of a rarely reported and possibly subclinical salmonella enterica serovar Derby strain. Appl. Environ. Microbiol. 86 (17).

Eveleigh, D., Lloyd, M., Hui, F., 2019. Using Armored RNA®/DNA as Reliable Molecular Controls in Infectious Disease Testing and Beyond. Asuragen Inc.

Gerrity, D., Papp, K., Stoker, M., Sims, A., Frehner, W., 2021. Early-pandemic wastewater surveillance of SARS-CoV-2 in southern Nevada: methodology, occurrence, and incidence/prevalence considerations. Water Res. X 10, 100086.

Graham, K.E., Loeb, S.K., Wolfe, M.K., Catoe, D., Sinnott-Armstrong, N., Kim, S., Yamahara, K.M., Sassoubre, L.M., Mendoza Grijalva, L.M., Roldan-Hernandez, L., Langenfeld, K., Wigginton, K.R., Boehm, A.B., 2021. SARS-CoV-2 RNA in wastewater settled solids is associated with COVID-19 cases in a large urban sewershed. Environ. Sci. Technol. 55 (1), 488–498.

Guan, W.-J., Ni, Z.-Y., Hu, Y., Liang, W.-H., Ou, C.-Q., He, J.-X., Liu, L., Shan, H., Lei, C.-L., Hui, D.S.C., Du, B., Li, L.-J., Zeng, G., Yuen, K.-Y., Chen, R.-C., Tang, C.-L., Wang, T., Chen, P.-Y., Xiang, J., Li, S.-Y., Wang, J.-L., Liang, Z.-J., Peng, Y.-X., Wei, L., Liu, Y., Hu, Y.-H., Peng, P., Wang, J.-M., Liu, J.-Y., Chen, Z., Li, G., Zheng, Z.-J., Qiu, S.-Q., Luo, J., Ye, C.-J., Zhu, S.-Y., Zhong, N.-S., 2020. Clinical characteristics of coronavirus disease 2019 in China. N. Engl. J. Med. 382 (18), 1708–1720.

Gupta, S., Parker, J., Smits, S., Underwood, J., Dolwani, S., 2020. Persistent viral shedding of SARS-CoV-2 in faeces - a rapid review. Color. Dis. 22 (6), 611–620.

Haramoto, E., Malla, B., Thakali, O., Kitajima, M., 2020. First environmental surveillance for the presence of SARS-CoV-2 RNA in wastewater and river water in Japan. Sci Total Environ 737 140405-140405.

Hasan, S.W., Ibrahim, Y., Daou, M., Kannout, H., Jan, N., Lopes, A., Alsafar, H., Yousef, A.F., 2021. Detection and quantification of SARS-CoV-2 RNA in wastewater and treated effluents: surveillance of COVID-19 epidemic in the United Arab Emirates. Sci. Total Environ. 764, 142929.

Havers, F.P., Reed, C., Lim, T., Montgomery, J.M., Klena, J.D., Hall, A.J., Fry, A.M., Cannon, D.L., Chiang, C.-F., Gibbons, A., Krapiunaya, I., Morales-Betoulle, M., Roguski, K., Rasheed, M.A.U., Freeman, B., Lester, S., Mills, L., Carroll, D.S., Owen, S.M., Johnson, J.A., Semenova, V., Blackmore, C., Blog, D., Chai, S.J., Dunn, A., Hand, J., Jain, S., Lindquist, S., Lynfield, R., Pritchard, S., Sokol, T., Sosa, L., Turabelidze, G., Watkins, S.M., Wiesman, J., Williams, R.W., Yendell, S., Schiffer, J., Thornburg, N.J., 2020. Seroprevalence of Antibodies to SARS-CoV-2 in 10 Sites in the United States, March 23-May 12, 2020. JAMA Intern. Med. 180 (12), 1576–1586.

He, X., Lau, E.H.Y., Wu, P., Deng, X., Wang, J., Hao, X., Lau, Y.C., Wong, J.Y., Guan, Y., Tan, X., Mo, X., Chen, Y., Liao, B., Chen, W., Hu, F., Zhang, Q., Zhong, M., Wu, Y., Zhao, L., Zhang, F., Cowling, B.J., Li, F., Leung, G.M., 2020. Temporal dynamics in viral shedding and transmissibility of COVID-19. Nat. Med. 26 (5), 672–675.

Hietala, S.K., Crossley, B.M., 2006. Armored RNA as virus surrogate in a real-time reverse transcriptase PCR assay proficiency panel. J. Clin. Microbiol. 44 (1), 67–70.

Hill, K., Zamyadi, A., Deere, D., Vanrolleghem, P.A., Crosbie, N.D., 2021. SARS-CoV-2 known and unknowns, implications for the water sector and wastewater-based epidemiology to support national responses worldwide: early review of global experiences with the COVID-19 pandemic. Water Qual. Res. J. Can. 56 (2), 57–67. https://doi.org/10.2166/wqrj.2020.100.

Hoffmann, T., Alsing, J., 2021. Faecal shedding models for SARS-CoV-2 RNA amongst hospitalised patients and implications for wastewater-based epidemiology. medRxiv 2021.2003.2016.21253603.

Hokajärvi, A.-M., Rytkönen, A., Tiwari, A., Kauppinen, A., Oikarinen, S., Lehto, K.-M., Kankaanpää, A., Gunnar, T., Al-Hello, H., Blomqvist, S., Miettinen, I.T., Savolainen-Kopra, C., Pitkänen, T., 2021. The detection and stability of the SARS-CoV-2 RNA biomarkers in wastewater influent in Helsinki, Finland. Science of The Total Environment 770, 145274.

Hokajärvi, A.M., Rytkönen, A., Tiwari, A., Kauppinen, A., Oikarinen, S., Lehto, K.M., Kankaanpää, A., Gunnar, T., Al-Hello, H., Blomqvist, S., Miettinen, I.T., Savolainen-Kopra, C., Pitkänen, T., 2021b. The detection and stability of the SARS-CoV-2 RNA biomarkers in wastewater influent in HelsinkiFinland. Sci Total Environ 770, 145274.

Hong, P.Y., Rachmadi, A.T., Mantilla-Calderon, D., Alkahtani, M., Bashawri, Y.M., Al Qarni, H., O'Reilly, K.M., Zhou, J., 2021. Estimating the minimum number of SARS-CoV-2 infected cases needed to detect viral RNA in wastewater: to what extent of the outbreak can surveillance of wastewater tell us? Environ. Res. 195, 110748.

Ing, A.J., Cocks, C., Green, J.P., 2020. COVID-19: in the footsteps of Ernest Shackleton. Thorax 75 (8), 693.

Ivanova, O.E., Yarmolskaya, M.S., Eremeeva, T.P., Babkina, G.M., Baykova, O.Y., Akhmadishina, L.V., Krasota, A.Y., Kozlovskaya, L.I., Lukashev, A.N., 2019. Environmental surveillance for poliovirus and other enteroviruses: long-term experience in Moscow, Russian Federation, 2004–2017. Viruses 11 (5), 424.

Jones, D.L., Baluja, M.Q., Graham, D.W., Corbishley, A., McDonald, J.E., Malham, S.K., Hillary, L.S., Connor, T.R., Gaze, W.H., Moura, I.B., Wilcox, M.H., Farkas, K., 2020. Shedding of SARS-CoV-2 in feces and urine and its potential role in person-to-person transmission and the environment-based spread of COVID-19. Sci. Total Environ. 749, 141364.

Kitajima, M., Ahmed, W., Bibby, K., Carducci, A., Gerba, C.P., Hamilton, K.A., Haramoto, E., Rose, J.B., 2020. SARS-CoV-2 in wastewater: state of the knowledge and research needs. Sci. Total Environ. 739, 139076.

Lauer, S.A., Grantz, K.H., Bi, Q., Jones, F.K., Zheng, Q., Meredith, H.R., Azman, A.S., Reich, N.G., Lessler, J., 2020. The incubation period of coronavirus disease 2019 (COVID-19) from publicly reported confirmed cases: estimation and application. Ann. Intern. Med. 172 (9), 577–582.

Li, Q., Guan, X., Wu, P., Wang, X., Zhou, L., Tong, Y., Ren, R., Leung, K.S.M., Lau, E.H.Y., Wong, J.Y., Xing, X., Xiang, N., Wu, Y., Li, C., Chen, Q., Li, D., Liu, T., Zhao, J., Liu, M., Tu, W., Chen, C., Jin, L., Yang, R., Wang, Q., Zhou, S., Wang, R., Liu, H., Luo, Y., Liu, Y., Shao, G., Li, H., Tao, Z., Yang, Y., Deng, Z., Liu, B., Ma, Z., Zhang, Y., Shi, G., Lam, T.T.Y., Wu, J.T., Gao, G.F., Cowling, B.J., Yang, B., Leung, G.M., Feng, Z., 2020. Early transmission dynamics in Wuhan, China, of novel coronavirus-infected pneumonia. N. Engl. J. Med. 382 (13), 1199–1207.

Manitoba, G.O., 2021. Manitoba COVID-19. https://experience.arcgis.com/experience/f55693e56018406ebbd08b3492e99771. https://experience.arcgis.com/experience/f55693e56018406ebbd08b3492e99771.

Markt, R., Mayr, M., Peer, E., Wagner, A.O., Lackner, N., Insam, H., 2021. Detection and stability of SARS-CoV-2 fragments in wastewater: impact of storage temperature. Pathogens 10 (9), 1215–1218. https://doi.org/10.3390/pathogens10091215.

McCall, C., Wu, H., Miyani, B., Xagoraraki, I., 2020. Identification of multiple potential viral diseases in a large urban center using wastewater surveillance. Water Res. 184, 116160.

Medema, G., Heijnen, L., Elsinga, G., Italiaander, R., Brouwer, A., 2020. Presence of SARS-Coronavirus-2 in sewage. medRxiv 2020.2003.2029.20045880.

Medema, G., Heijnen, L., Elsinga, G., Italiaander, R., Brouwer, A., 2020b. Presence of SARS-Coronavirus-2 RNA in sewage and correlation with reported COVID-19 prevalence in the early stage of the epidemic in the Netherlands. Environ. Sci. Technol. Lett. 7 (7), 511–516.

Nakamura, T., Hamasaki, M., Yoshitomi, H., Ishibashi, T., Yoshiyama, C., Maeda, E., Sera, N., Yoshida, H., 2015. Environmental surveillance of poliovirus in sewage water around the introduction period for inactivated polio vaccine in Japan. Appl. Environ. Microbiol. 81 (5), 1859–1864.

Nghiem, L.D., Morgan, B., Donner, E., Short, M.D., 2020. The COVID-19 pandemic: considerations for the waste and wastewater services sector. Case Studies in Chemical and Environmental Engineering. 1.

Pan, Y., Zhang, D., Yang, P., Poon, L.L.M., Wang, Q., 2020. Viral load of SARS-CoV-2 in clinical samples. Lancet Infect. Dis. 20 (4), 411–412.

Parsa, S.M., Momeni, S., Hemmat, A., Afrand, M., 2021. Effectiveness of solar water disinfection in the era of COVID-19 (SARS-CoV-2) pandemic for contaminated water/wastewater treatment considering UV effect and temperature. J. Water Process Eng. 43, 102224.

Peccia, J., Zulli, A., Brackney, D.E., Grubaugh, N.D., Kaplan, E.H., Casanovas-Massana, A., Ko, A.I., Malik, A.A., Wang, D., Wang, M., Warren, J.L., Weinberger, D.M., Arnold, W., Omer, S.B., 2020. Measurement of SARS-CoV-2 RNA in wastewater tracks community infection dynamics. Nat. Biotechnol. 38 (10), 1164–1167.

Philo, S.E., Keim, E.K., Swanstrom, R., Ong, A.Q.W., Burnor, E.A., Kossik, A.L., Harrison, J.C., Demeke, B.A., Zhou, N.A., Beck, N.K., Shirai, J.H., Meschke, J.S., 2021. A comparison of SARS-CoV-2 wastewater concentration methods for environmental surveillance. Sci. Total Environ. 760, 144215.

Randazzo, W., Truchado, P., Cuevas-Ferrando, E., Simón, P., Allende, A., Sánchez, G., 2020. SARS-CoV-2 RNA in wastewater anticipated COVID-19 occurrence in a low prevalence area. Water Res. 181 115942-115942.

Rose, C., Parker, A., Jefferson, B., Cartmell, E., 2015. The characterization of feces and urine: a review of the literature to inform advanced treatment technology. Crit. Rev. Environ. Sci. Technol. 45 (17), 1827–1879.

Saawarn, B., Hait, S., 2021. Occurrence, fate and removal of SARS-CoV-2 in wastewater: current knowledge and future perspectives. J Environ Chem Eng 9 (1) 104870-104870.

Sala-Comorera, L., Reynolds, L.J., Martin, N.A., O'Sullivan, J.J., Meijer, W.G., Fletcher, N.F., 2021. Decay of infectious SARS-CoV-2 and surrogates in aquatic environments. Water Res. 201, 117090.

Sherchan, S.P., Shahin, S., Ward, L.M., Tandukar, S., Aw, T.G., Schmitz, B., Ahmed, W., Kitajima, M., 2020. First detection of SARS-CoV-2 RNA in wastewater in North America: A study in Louisiana, USA. Sci Total Environ 743 140621-140621.

Simpson, A., Topol, A., White, B.J., Wolfe, M.K., Wigginton, K.R., Boehm, A.B., 2021. Effect of storage conditions on SARS-CoV-2 RNA quantification in wastewater solids. PeerJ 9, e11933.

Sulej-Suchomska, A.M., Klupczynska, A., Dereziński, P., Matysiak, J., Przybyłowski, P., Kokot, Z.J., 2020. Urban wastewater analysis as an effective tool for monitoring illegal drugs, including new psychoactive substances, in the eastern european region. Sci. Rep. 10 (1), 4885.

Thompson, J.R., Nancharaiah, Y.V., Gu, X., Lee, W.L., Rajal, V.B., Haines, M.B., Girones, R., Ng, L.C., Alm, E.J., Wuertz, S., 2020. Making waves: Wastewater surveillance of SARS-CoV-2 for population-based health management. Water Res 184 116181-116181.

Uyaguari-Diaz, M.I., Chan, M., Chaban, B.L., Croxen, M.A., Finke, J.F., Hill, J.E., Peabody, M.A., Van Rossum, T., Suttle, C.A., Brinkman, F.S.L., Isaac-Renton, J., Prystajecky, N.A., Tang, P., 2016. A comprehensive method for amplicon-based and metagenomic characterization of viruses, bacteria, and eukaryotes in freshwater samples. Microbiome 4 (1), 20.

Wang, Z., Yang, W., Hua, P., Zhang, J., Krebs, P., 2021. Transmission risk of SARS-CoV-2 in the watershed triggered by domestic wastewater discharge. Sci. Total Environ. 150888.

Wei, W.E., Li, Z., Chiew, C.J., Yong, S.E., Toh, M.P., Lee, V.J., 2020. Presymptomatic transmission of SARS-CoV-2 - Singapore, january 23-march 16, 2020. MMWR Morb. Mortal. Wkly Rep. 69 (14), 411–415.

Westhaus, S., Weber, F.-A., Schiwy, S., Linnemann, V., Brinkmann, M., Widera, M., Greve, C., Janke, A., Hollert, H., Wintgens, T., Ciesek, S., 2021. Detection of SARS-CoV-2 in raw and treated wastewater in Germany – suitability for COVID-19 surveillance and potential transmission risks. Sci. Total Environ. 751, 141750.

<collab>Winnipeg, T.C.o</collab>, 2021. Population of Winnipeg, The City of Winnipeg. . https://winnipeg.ca/cao/pdfs/population.pdf.

Wölfel, R., Corman, V.M., Guggemos, W., Seilmaier, M., Zange, S., Müller, M.A., Niemeyer, D., Jones, T.C., Vollmar, P., Rothe, C., Hoelscher, M., Bleicker, T., Brünink, S., Schneider, J., Ehmann, R., Zwirglmaier, K., Drosten, C., Wendtner, C., 2020. Virological assessment of hospitalized patients with COVID-2019. Nature 581 (7809), 465–469.

Wu, F., Xiao, A., Zhang, J., Moniz, K., Endo, N., Armas, F., Bonneau, R., Brown, M.A., Bushman, M., Chai, P.R., Duvallet, C., Erickson, T.B., Foppe, K., Ghaeli, N., Gu, X., Hanage, W.P., Huang, K.H., Lee, W.L., Matus, M., McElroy, K.A., Nagler, J., Rhode, S.F., Santillana, M., Tucker, J.A., Wuertz, S., Zhao, S., Thompson, J., Alm, E.J., 2022. SARS-CoV-2 RNA concentrations in wastewater foreshadow dynamics and clinical presentation of new COVID-19 cases. Sci. Total Environ. 805, 150121.

Wu, S.L., Mertens, A.N., Crider, Y.S., Nguyen, A., Pokpongkiat, N.N., Djajadi, S., Seth, A., Hsiang, M.S., Colford, J.M., Reingold, A., Arnold, B.F., Hubbard, A., Benjamin-Chung,

J., 2020. Substantial underestimation of SARS-CoV-2 infection in the United States. Nat. Commun. 11 (1), 4507.
Wurtzer, S., Waldman, P., Ferrier-Rembert, A., Frenois-Veyrat, G., Mouchel, J.M., Boni, M., Maday, Y., Marechal, V., Moulin, L., 2021. Several forms of SARS-CoV-2 RNA can be detected in wastewaters: implication for wastewater-based epidemiology and risk assessment. Water Res. 198, 117183.
Yan, T., O'Brien, P., Shelton, J.M., Whelen, A.C., Pagaling, E., 2018. Municipal wastewater as a microbial surveillance platform for enteric diseases: a case study for salmonella and salmonellosis. Environ. Sci. Technol. 52 (8), 4869–4877.
Ye, Y., Ellenberg, R.M., Graham, K.E., Wigginton, K.R., 2016. Survivability, partitioning, and recovery of enveloped viruses in untreated municipal wastewater. Environ. Sci. Technol. 50 (10), 5077–5085.
Zaneti, R.N., Girardi, V., Spilki, F.R., Mena, K., Westphalen, A.P.C., da Costa Colares, E.R., Pozzebon, A.G., Etchepare, R.G., 2021. Quantitative microbial risk assessment of SARS-CoV-2 for workers in wastewater treatment plants. Sci. Total Environ. 754, 142163.